PRIMORDIAL NON-GAUSSIANITY AND EXCURSION SETS

Graziano Rossi, with Pravabati Chingangbam and Changbom Park

Korea Institute for Advanced Study (KIAS), School of Physics, Dongdaemun-gu, Seoul 130-722, KR

ABSTRACT

We use the statistics of regions above or below a temperature threshold (excursion sets) to study the cosmic microwave background (CMB) anisotropy in models with primordial non-Gaussianity of the local type. By computing the full-sky spatial distribution and clustering of pixels above/below threshold from a large set of simulated maps with different levels of non-Gaussianity, we find that a positive value of the dimensionless non-linearity parameter $f_{\rm NL}$ enhances the number density of the cold CMB excursion sets along with their clustering strength, and reduces that of the hot ones. We quantify the robustness of this effect, which may be important to discriminate between the simpler Gaussian hypothesis and non-Gaussian scenarios, arising either from non-standard inflation or alternative early-universe models. The clustering of hot and cold pixels exhibits distinct non-Gaussian signatures, particularly at angular scales of about 75 arcmin (i.e. around the Doppler peak), which increase linearly with $f_{\rm NL}$. Moreover, the clustering changes strongly as a function of the smoothing angle. We propose several statistical tests to maximize the detection of a local primordial non-Gaussian signal, and provide some theoretical insights within this framework, including an optimal selection of the threshold level. We also describe a procedure which aims at minimizing the cosmic variance effect, the main limit within this statistical framework.

THEORETICAL FRAMEWORK

Given a CMB map with a temperature assigned to each point, an excursion set is the ensemble of all pixels with temperatures greater than a fixed threshold. The complementary excursion set for temperatures lesser than a given level is symmetrically defined; in the Gaussian case, it is expected to give the same results as the corresponding hot excursion set. Instead, peculiar asymmetries arise in the presence of non-Gaussianity of the local $f_{\rm NL}$-type. For example, the number density of regions above (below) a temperature threshold $\nu = \delta T/\sigma$, with σ being the rms of the map, becomes:

$$n_{\rm pix}^{\rm NG}(\nu) = n_{\rm pix}^{\rm G}(\nu) + n_{\rm pix}^{\rm f_{NL}}(\nu) = \frac{N_{\rm pix,tot}}{4\pi}\cdot\left\{\frac{{\rm erfc}(\nu/\sqrt{2})}{2} + \frac{\sigma S^{(0)}}{6\sqrt{2\pi}}(\nu^2-1)e^{-\nu^2/2}\right\} \quad (1)$$

where $N_{\rm pix,tot} = 12N_{\rm side}^2$ is the total number of pixels in the map, at a resolution specified by the parameter $N_{\rm side}$. The skewness parameter $S^{(0)} \equiv \langle\delta T^3\rangle/\sigma^4$ needs to be evaluated numerically; it contains the reduced bispectrum specific to the non-Gaussian model. Equation (1) implies that the underlying one-dimensional PDF in presence of local non-Gaussianity is given by:

$$p(\nu){\rm d}\nu \approx \frac{1}{\sqrt{2\pi}}e^{-\nu^2/2}\left\{1 + \frac{\sigma S^{(0)}}{6}\nu(\nu^2-3)\right\}{\rm d}\nu. \quad (2)$$

The correlation of the excursion sets above $\bar{\nu}$ is instead (Kaiser 1984):

$$1 + \xi_{\bar{\nu}}(\theta) = P_2/P_1^2 = \int_{\bar{\nu}}^{\infty} p(\nu){\rm d}\nu \Big/ \Big[\int_{\bar{\nu}}^{\infty}{\rm d}\nu_1\int_{\bar{\nu}}^{\infty}{\rm d}\nu_2\, p(\nu_1,\nu_2,w)\Big]^2 \quad (3)$$

with $p(\nu_1,\nu_2,w)$ being the two-dimensional PDF and $w \equiv w(\theta) = \langle\nu_1\nu_2\rangle$ the correlation. In the case of weak non-Gaussianity, equation (2) must be used in the previous expression, and for $p(\nu_1,\nu_2,w)$ we expect a bivariate Edgeworth expansion to provide a reasonably good description at low thresholds:

$$p(\nu_1,\nu_2,w){\rm d}\nu_1{\rm d}\nu_2 \approx \frac{1}{2\pi\sqrt{1-w^2}}\exp\left\{-\frac{\nu_1^2+\nu_2^2-2\nu_1\nu_2 w}{2(1-w^2)}\right\}\times\left[1+\sigma S^{(0)}\Big(\frac{H_{30}+H_{03}}{6}\Big)+\lambda\Big(\frac{H_{21}+H_{12}}{2}\Big)\right]{\rm d}\nu_1{\rm d}\nu_2 \quad (4)$$

where $\lambda = \langle\nu_1^2\nu_2\rangle \equiv \langle\nu_1\nu_2^2\rangle$ and

$$H_{30}(\nu_1,\nu_2,w) = H_{03}(\nu_2,\nu_1,w)\frac{(\nu_1-w\nu_2)^3}{(1-w^2)^3} - \frac{3(\nu_1-w\nu_2)}{(1-w^2)^2}, \quad (5)$$

$$H_{21}(\nu_1,\nu_2,w) = H_{12}(\nu_2,\nu_1,w)\frac{2w(\nu_1-w\nu_2)-(\nu_2-w\nu_1)}{(1-w^2)^2} + \frac{(\nu_2-w\nu_1)(\nu_1-w\nu_2)^2}{(1-w^2)^3}. \quad (6)$$

NON-GAUSSIAN SIMULATIONS

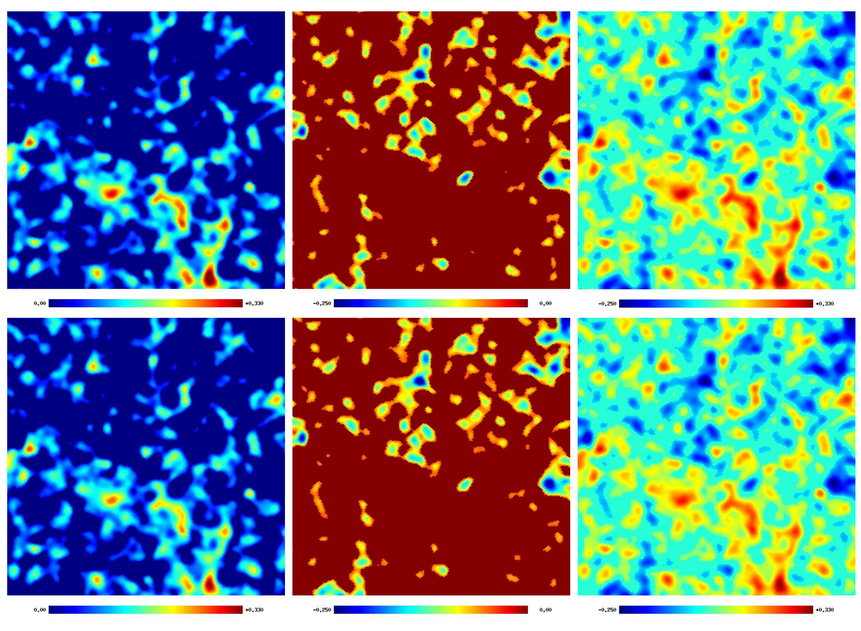

Figure 1. A small patch ($\simeq 10^\circ\times10^\circ$) of the simulated CMB sky with primordial Gaussianity (top panels) and non-Gaussianity of the local type with $f_{\rm NL} = 500$ (bottom panels), when smoothed with a Gaussian beam of FWHM=30 arcmin. Regions below the threshold $\nu = 0.50$ (left panels), above $\nu = -0.50$ (middle panels), or above and below the considered threshold (right panels) are set to zero. The temperature scale is in mK, ranging from -0.250 to +0.330.

- Simulations of the full CMB sky at $N_{\rm side} = 512$, with $N_{\rm pix} = 3145728$, separated on average by $\theta_{\rm pix} = 6.87$ arcmin and constructed as explained in Chingangbam & Park (2009).
- Different values of $f_{\rm NL}$ considered, over a range of Gaussian smoothing angles.
- The pipeline involves the correct assignment pixels $\rightarrow$ *HEALPix* coordinates, and the selection of pixels above/below a temperature threshold.

MAIN RESULTS

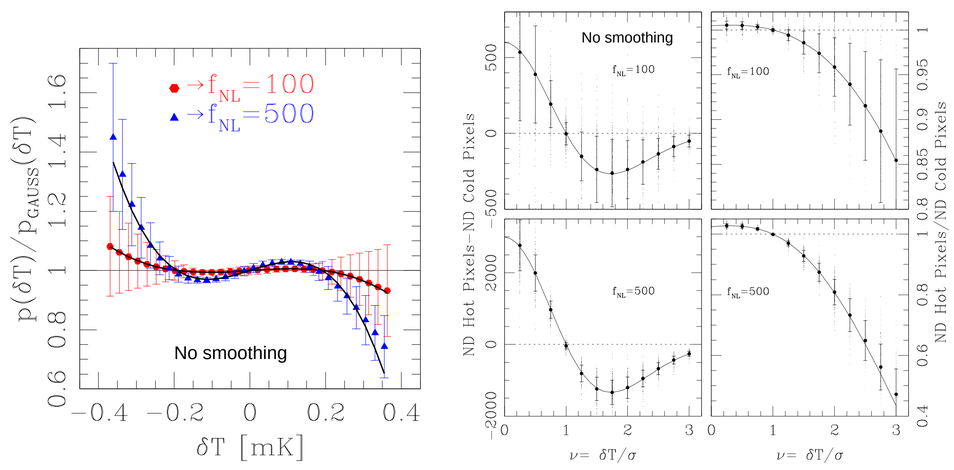

Figure 2. [Left] CMB temperature distribution (mK units) in the presence of weak local non-Gaussianity, when no smoothing is applied. Points in the panel are averages over 200 non-Gaussian simulations with $f_{\rm NL} = 100$ and 500; errorbars are the corresponding 1σ run-to-run estimates, and solid lines are from equation (2) for the two different $f_{\rm NL}$ values. The average rms of δT is 0.111 mK. [Right] Difference and ratio between hot and cold excursion set regions, at corresponding temperature thresholds, when no smoothing is applied. In the top panels $f_{\rm NL} = 100$, in the bottom ones $f_{\rm NL} = 500$. Solid lines are theoretical expectations derived from equation (1). At $\nu = 1$, a transition area in the number density is clearly visible.

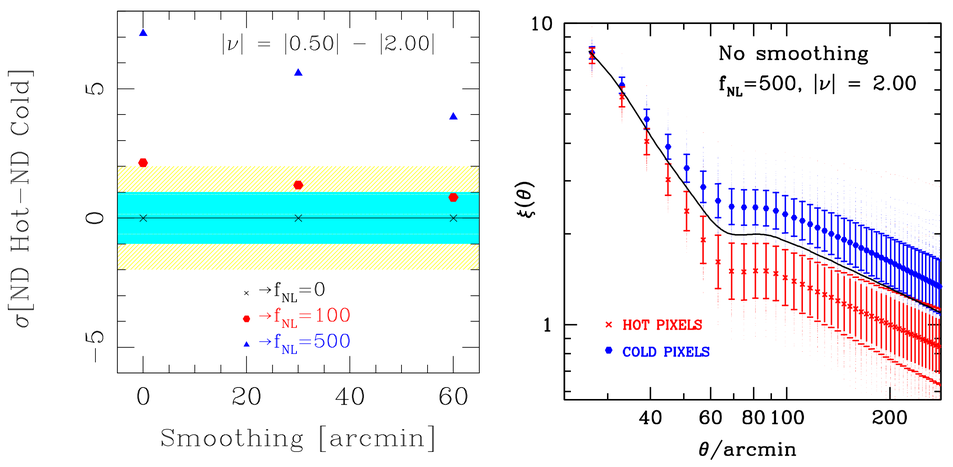

Figure 3. [Left] Composite quantity for the pixel number density, as a function of the smoothing scale. The panel is in rms units, with errorbars estimated from 200 realizations. The two areas where the non-Gaussian sensitivity is maximized, $|\nu| = 0.50$ and $|\nu| = 2.00$, are combined in order to boost the departure from Gaussianity. [Right] Clustering strength of pixels above/below threshold when $|\nu| = 2.00$, a regime particularly sensitive to a non-Gaussian signal of the local $f_{\rm NL}$-type. The panel represents the case of $f_{\rm NL} = 500$, when no smoothing is applied. The solid line is the analytic prediction in the Gaussian limit.

WORK IN PROGRESS

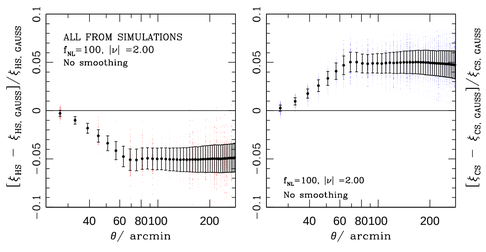

Figure 4. Statistical test which involves the clustering information alone. Measurements of the relative clustering strength from the non-Gaussian simulations for hot (left) and cold (right) excursion set regions, with the Gaussian predictions $\xi_{\nu,\rm Gauss}^{\rm NG}$ computed from the corresponding Gaussian maps with the same random seeds of the non-Gaussian ones. In this way, the cosmic variance effect is completely cancelled.

- Since cosmic variance is the main obstacle in the analysis, we are considering derived statistics which could potentially beat its effect and maximize the non-Gaussian contribution.
- Including realistic effects in our simulations, such as inhomogeneous noise, point source contamination or foregrounds, so that we can compare our predictions with current observations, is subject of ongoing work.
- Application of the formalism presented here to peak rather than pixel statistics is a straightforward exercise, and is also the subject of another forthcoming publication.
- Repeating this analysis at the Planck resolution may provide more stringent limits on $f_{\rm NL}$ from the excursion set statistics, and is also the subject of work in progress.

Selected References

- Rossi, G., Chingangbam, P. & Park, C. 2010, MNRAS (arXiv: 1003.0272)
- Rossi, G., Sheth, R. K., Park, C., & Hernández-Monteagudo, C. 2009, MNRAS, 399, 304
- Chingangbam, P., & Park, C. 2009, JCAPP, 12, 19